Simplified Modeling of Cross-Ventilation Airflow

Guilherme Carrilho da Graça
Student Member ASHRAE

P.F. Linden, Ph.D.
Associate Member ASHRAE

ABSTRACT

This paper presents a study of room cross-ventilation airflow. A simplified model is developed using scaling analysis, experimental correlations, and computational fluid dynamics. The model distinguishes two regions in the room, the main jet region and the recirculations, and models relevant flow features that are essential inputs when predicting heat and pollutant transfers as well as indoor thermal comfort conditions. The results of the model are a set of formulas that predict the airflow rates and characteristic velocities in the jet and recirculation flow regions. The formulas clearly display the first order effects of room geometry on cross-ventilation airflow characteristics. Simple examples of application of the model to cross-ventilation design are presented.

INTRODUCTION

Buildings are often designed using energy-inefficient indoor climate control systems. This approach is made possible through intensive use of HVAC equipment. To mitigate these problems, naturally driven cooling systems can be employed. In these cases, air movement through the building is driven by buoyancy forces, or the wind, or a combination of the two.

Modern building systems performance standards create a need for accurate and flexible simulation models. Developing improved models is critical to increased use of low energy or naturally driven cooling. In these systems, the cooling power is variable and often small, making performance simulation and consequent design decisions more challenging and critical to overall success.

The three most commonly used room ventilation strategies are: mixing ventilation, displacement, and cross-ventilation (C-V). Mixing ventilation systems are used in most air-conditioned buildings, where cool inflow air introduced through vents near the ceiling mixes with room air, and the resultant momentum diffusion leads to the absence of a preferred direction for air motion in the room. In displacement ventilation systems, the predominant air movement is vertical, due to buoyancy production by internal heat sources, typically with low momentum fluxes and small horizontal movements across the room. Both of these ventilation flows are in contrast with C-V, where significant conservation of inflow momentum occurs with the inlet airflow traveling freely across the room. Poorly designed mixing ventilation systems can exhibit C-V characteristics, with undesirable short-circuiting between inlet and outlet. ASHRAE (2001) classifies this type of flow as entrainment flow. Cross-ventilated rooms with recirculation regions fit the ASHRAE definition of entrainment flow and can exhibit the characteristic poor mixing between different zones in the room.

Because of the high momentum conservation, C-V configurations are often used when there is need for high ventilation airflow rates. Flows that occur in many naturally ventilated buildings belong to this category, with air flowing through windows, open doorways, and large internal apertures across rooms and corridors inside the building. This also occurs in many industrial mechanical ventilation systems and hybrid ventilation systems, for both direct heat and pollutant removal and nighttime structural cooling.

Figure 1 shows a schematic plan view of a cross-ventilated room with internal gains and thermally active internal surfaces. In order to model heat and pollutant transfer and to evaluate thermal comfort, two interrelating components of the C-V system must be modeled. These components are the

Guilherme Carrilho da Graça is a research assistant and **Paul F. Linden** is a professor at the University of California, San Diego, La Jolla, Calif.

THIS PREPRINT IS FOR DISCUSSION PURPOSES ONLY, FOR INCLUSION IN ASHRAE TRANSACTIONS 2003, V. 109, Pt. 1. Not to be reprinted in whole or in part without written permission of the American Society of Heating, Refrigerating and Air-Conditioning Engineers, Inc., 1791 Tullie Circle, NE, Atlanta, GA 30329. Opinions, findings, conclusions, or recommendations expressed in this paper are those of the author(s) and do not necessarily reflect the views of ASHRAE. Written questions and comments regarding this paper should be received at ASHRAE no later than **February 7, 2003**.

airflow pattern (light gray arrows in Figure 1) and determining the magnitude of the local transfers of heat and pollutants between the airflow in its different paths, the internal surfaces, and the internal sources (dark gray arrows in Figure 1).

Each of the two parts of the problem poses considerable challenge. By definition, any ventilation airflow pattern has an element of direct air movement between inlet and outlet, but, as will be clear below, in some regions of the room, air can move in other directions. In the local heat and pollutant transfer part of this problem, it is clear from conservation principles that all convective and advective transfers from room surfaces and internal sources will, at one point in the ventilation process, be transferred to the airflow. Transfers between airflow and the internal sources depend on the local concentration gradient and transfer coefficient. In particular, when modeling heat transfer, it is relevant to determine how much energy from the internal gains is transferred to the internal surfaces and not exhausted by the ventilation air. Clearly, room ventilation transfer problems are composed of two sub-problems that connect in a more or less complex way depending on the ventilation system and room geometry. The model described in this paper will address the airflow pattern component of the C-V modeling problem.

Existing Approaches

In order to predict airflow characteristics in C-V, there are currently three available options: computational fluid dynamics (CFD, typically using Reynolds averaged turbulence models), zonal models, and experimental correlations.

The use of CFD requires extensive expertise and time. Further, in many design situations, the precision level and amount of information required and provided can be excessive. Often in these cases the building geometry is not fully defined, making simple modeling approaches and results more adequate than complex flow field simulations. Further, in many situations, designers need to analyze multi-room ventilation geometries using weather data spanning several days or months. In these cases, the use of CFD is impractical and simpler ventilation models are more adequate.

Zonal models simulate indoor airflow by solving for mass and momentum conservation in a set of zones (often fewer than twenty). These models generally require user identification of the dominant room airflow components (jets, boundary layers, plumes, etc.) that are "contained" in particular zones. Because the momentum equation is not solved in the iteration procedure, an artificial flow resistance is imposed between room zones (Allard and Inard 1992). These features make these models imprecise and often complex to use. As shown below, the model presented in this paper does not impose artificial flow resistances and does not require numerical iteration.

Experimental correlations provide a way to model complex ventilation systems such as C-V of rooms (Givoni 1976; Aynsley et al. 1977; Ernst et al. 1991). However, because these correlations are obtained for particular geometries, they lack flexibility to handle variable room geometries.

From a fundamental point of view, all of these approaches fail to provide simple insights into the mechanisms and system parameters that control the C-V airflow pattern. As mentioned above, high precision may not be required for the design of a cross-ventilated room or building. Simplicity and qualitative identification of the most relevant room geometry parameters and their influence in the airflow pattern are more relevant. As a consequence of the complexity of the problem and the simple solution approach that will be used, first order precision is expected and considered acceptable in view of other uncertainties that are common in building ventilation design, such as furniture geometry, building use, and outside weather conditions.

DEFINING THE AIRFLOW PATTERN

The left side of Figure 2 shows a simple room geometry that can lead to C-V, with an inlet window facing an identical outlet on an opposing room surface. To develop a simple model for airflow in this type of room, it is necessary to make approximations that will allow for a simple analysis while retaining the ability to model the dominant characteristics of the problem. Achieving this goal in the present case requires the use of two types of approximations: in the characterization of the physical processes and in the system geometry.

The main approximations in the system geometry are the following:

1. The model is restricted to rectangular rooms with flat surfaces.
2. Air enters the room through one aperture and leaves through an aperture located in the opposing vertical surface (as shown in Figure 2).
3. The effects of furniture are not considered in detail.
4. The effects of variations in outlet geometry are neglected.

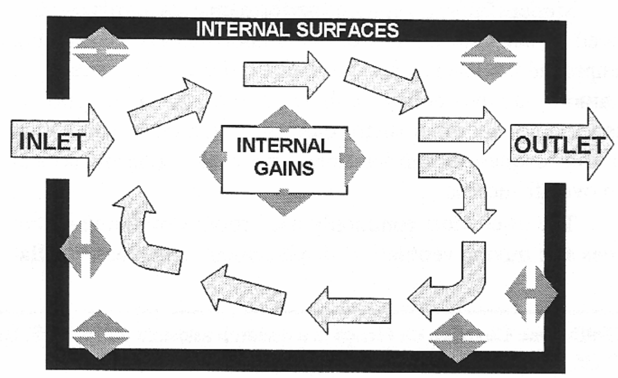

Figure 1 *Schematic plan view of a cross-ventilated room. Dark gray arrows represent heat flow; light gray arrows represent airflow.*

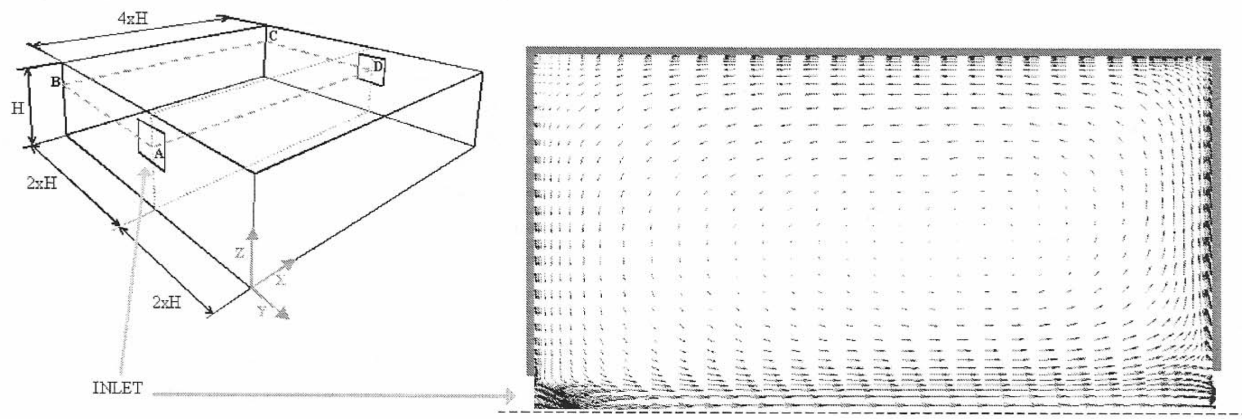

Figure 2 *Left: Basic compartment geometry considered in the model (case W144 in Table 3). Right: Top view of one-half of the velocity field, result of a CFD simulation using the geometry on the left (taking advantage of the system symmetry to simulate only one-half of the room volume).*

With regard to 4, Baturin and Billington (1972) show experimental evidence of the small magnitude of the effects of outlet geometry, confirmed in the CFD simulations presented below. With these approximations, only five parameters are needed to characterize the room geometry: width (W), height (H), length (L), area (A_{IN}) of the inlet aperture, and position of the inlet aperture (close to the center or close to the perimeter of the inlet surface).

We begin the analysis of the approximations used in the physical processes with a discussion of the flow regime, a fundamental question when defining the flow pattern. C-V airflows can be seen as an interaction between several "flow elements": a jet, flat surface boundary layers, and shear layers. All of these flow elements have been studied in detail in the past and their basic behavior can be predicted using simple physical models or correlations. It is then necessary to identify these elements in the C-V flow and determine the flow regimes in which they occur.

C-V flows tend to be turbulent in most regions of the room. The main system features that contribute to this turbulence dominated flow are:

- large characteristic room dimensions (typical room length (L) around 5-15 m), combined with flow velocities close to the inlet aperture that typically vary between 0.2 and 2 m/s;
- the existence of turbulent "flow elements" interacting in a confined space, such as the shear layers that begin at the edge of the inlet aperture and expand as the air travels toward the outlet and the boundary layers that occur close to the room surfaces (see Figure 2);
- significant velocities close to the room surfaces (0.1-1 m/s). These velocities are generally higher than those commonly found in rooms with HVAC systems.

The shear layers that typically occur in room airflow have a small laminar region (smaller than 0.1 m [Bejan 1994]). In horizontal forced convection boundary layers, transition to turbulence occurs within the first one-half meter (for a forced flow free stream velocity of 0.1 m/s or higher). Additional sources of turbulence are: jets impinging on room surfaces, flow around furniture, room corners, and most internal heat sources (generation of turbulence through buoyancy induced flow). Between the different flow elements that can occur in C-V, there may be regions of light shear, almost stagnant flow. Because most of the momentum transfer occurs in turbulent regions, the flow is dominated by turbulent processes and regions of laminar flow will not be modeled explicitly. However, the presence of these laminar regions is considered implicitly, since, due to the lower momentum transfer that characterizes them, they form boundaries that establish the spatial limits of the main flow regions.

The C-V flows to which the model applies are bounded by a stationary geometry, have fixed airflow rates, and are dominated by horizontal momentum flux, as opposed to buoyancy dominated (which typically occurs in displacement ventilation). For ventilation systems with these characteristics, if the flow regime is stable (predominantly turbulent, as discussed above), the flow pattern will be steady, approximately self similar, and suitable for the application of scaling analysis principles. As a consequence, all the velocities in the room are expected to scale linearly with the characteristic velocity of the inlet flow:

$$U_R = C_n \cdot F(L, W, H, A_{IN}, \ldots) \cdot U_{IN} \tag{1}$$

The function F is expected to depend on L, W, H, A_{IN}, and inlet location. The velocity scale U_{IN} of the inlet jet will be defined by

$$M = \int_{A_{IN}} \rho \cdot (U_{MAX} \cdot f(\vec{r}))^2 \, dA, \qquad U_{IN} = \sqrt{M/\rho A_{IN}}, \quad (2)$$

where $f(\vec{r})$ is a function that models the inflow profile.

In order to correlate the velocities in different regions of the room, the corresponding correlation constants C_n and scaling laws F must be obtained. By multiplying the velocities in (1) by suitable areas, correlations for flow rates can be obtained. The remainder of this section focuses on defining the flow pattern.

The Three Types of Flow Pattern

Figure 3 shows a schematic representation of the three basic airflow patterns that can occur in C-V. Any cross-ventilated room will have an airflow pattern that is either similar to one of the two base cases shown in Figure 3 (cases C and R), or a combination of the two with both recirculation and inlet flow attaching to a lateral surface or the ceiling (case CR).

The simplest flow configuration, case C, commonly occurs in corridors and long spaces whose inlet aperture area is similar to the room cross-sectional area. In this case, the flow occupies the full cross section of the room, and the transport of pollutants and momentum is unidirectional, similar to turbulent flow in a channel. The flow velocity profile across the channel is approximately flat due to the high degree of mixing that is characteristic of turbulent flows. The average airflow velocity in the cross section can be obtained approximately by dividing the flow rate by the cross-sectional area of the space.

A more complicated airflow pattern occurs when the inlet aperture area is an order of magnitude smaller than the cross-sectional area of the room $A_R = W \cdot H$ (for the case shown in Figure 2, $A_R = 4 \cdot H^2$). In these cases, the main C-V region in the core of the room entrains air from the adjacent regions and forms recirculations that ensure mass conservation, with air moving in the opposite direction to the core jet flow in some regions of the room (see cases R and CR in Figure 3). These recirculating flow regions have been observed in many experiments. The most relevant to the present problem are Aynsley et al. (1976), Baturin et al. (1972), Neiswanger et al. (1987), and Ohba et al. (2001). For these room geometries, when the inlet is located close to the center of the inlet surface, most of the contact between ventilation flow and the internal surfaces occurs in the recirculation regions that occupy the majority of the room volume.

A set of CFD simulations (to be described below), based on geometry similar to Figure 2, confirmed the relation between the nondimensional coefficient,

$$A^* = A_R / A_{IN}, \quad (3)$$

and the flow pattern. Based on this coefficient it is possible to distinguish the three cases presented in Figure 3:

Case C, $A^* \cong 1$: the flow attaches to the room surfaces and is similar to turbulent flow in a channel.

Case R, $A^* \gg 1$: the flow can be divided in two regions: the jet region, connecting the inlet and the outlet and the recirculation region, composed of the return flow that occurs along the cross-flow perimeter of the room. In the recirculation region, the maximum velocity occurs close to the internal surfaces and the flow is similar to an attached jet (a wall jet).

Case CR, $A^* \cong 2$: a combination of cases R and C. The jet flow attaches to part of the room perimeter, as in case C; still, in most cases the recirculation flow occupies the majority of the room volume.

Most rooms have inlets that are almost one order of magnitude smaller than the room cross section, resulting in a flow pattern closer to case R or CR. Since the characterization of the flow in case C is straightforward, the following analysis will discuss geometries of type R. These geometries present a considerable challenge because in these cases the transport of heat and pollutants is not unidirectional and there is no analytical solution for the room airflow pattern.

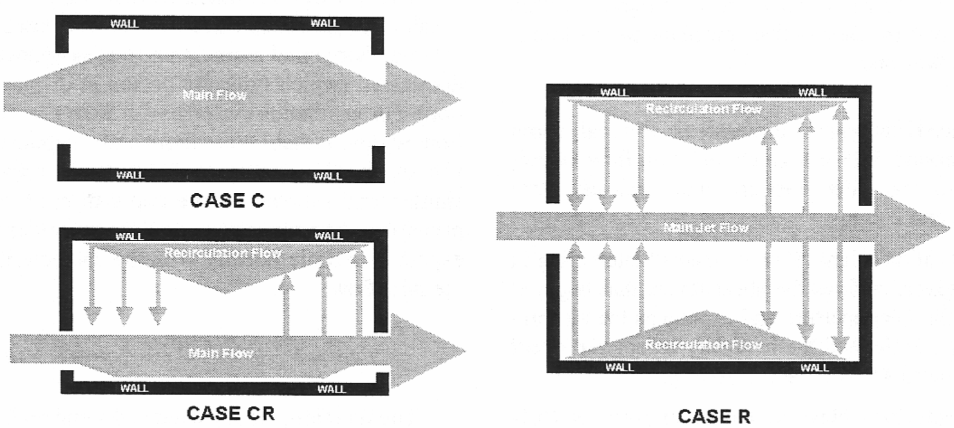

Figure 3 *Top view of the three possible airflow patterns in cross-ventilation.*

Characterization of the Flow in the Recirculation Regions

As a first step, we analyze the CFD-generated velocity field in the horizontal plane of a cross-ventilated room, shown in Figure 2. The flow in the recirculation regions is composed by wall "currents" resembling attached jets that form close to the outlet and are re-entrained in the first half of the path of the inflow jet in the room. These wall currents are bounded by a boundary layer in the region adjacent to the internal surfaces and, as will be shown below, are subject to pressure gradients that are a consequence of the presence of the inflow jet in a confined space. Because there is no analytic solution for the flow field in the room, the need for a correlation arises as a simple solution to account for room confinement and energy dissipation effects. In the process of developing the correlation, the dominant physical processes in this flow will be identified and modeled.

The recirculation regions are a fundamental part of this C-V flow. The flow rate in the recirculation region determines the capacity of the recirculating flow to absorb and release heat and pollutants without significant concentration variations. Predicting the velocities in the main jet and recirculation regions is essential to estimating comfort and meeting particular design goals (such as maximum and minimum indoor velocities). Due to the importance of jets in the airflow pattern, it is useful to review here the most relevant aspects of jet flow for the present problem.

Characterization of the Flow in the Jet Region

The jets that occur in C-V are approximately axisymmetric for most of the propagation path in the room as long as there is no contact with a room surface. Whenever the jet is close to a room surface, attachment occurs and a wall jet is generated. The velocity scale of the jets can be adequately represented by the average inlet velocity ($U_{JET} \approx U_{IN}$, see Equation 2), and the characteristic diameter is $\approx \sqrt{A_{IN}}$.

Jets entrain ambient fluid throughout the propagation path leading to a continuous increase of the transported mass flow rate. In the initial part of the propagation path, a jet is essentially a shear layer that develops along the perimeter of the inlet aperture. When the shear layer reaches the center of the jet, so that it occupies it fully, the jet enters the transition stage and a self-similar, Gaussian velocity profile is formed. This transition stage is initiated between 4 to 8 diameters from the inlet and ends at around 20 diameters (Tennekes and Lumley 1994; Malmstrom et al. 1997). In the transition stage, the amplitude of the jet starts to decay.

Because most building apertures have diameters of at least one meter, most jets that occur in C-V do not reach the transition stage in the room (this is the case for the jet shown in Figure 2), possibly reaching the beginning of this transition stage for very long rooms. Most common building apertures, such as doors and windows (not preceded by a corridor with the same section as the aperture), result in an inlet flow that has significant radial velocity due to flow convergence just before the inlet. This is distinct from the square, two-dimensional inflow velocity profile that is characteristic of experiments with jets. Still, the jets that occur in C-V flows have shear layers developing from the inlet and a nearly square inlet velocity profile (in the vena contracta region that occurs after the inlet). Further, it will become clear below that any effects from non-square velocity profiles that may exist in the flow are considered in the correlation process by using an integral analysis in conjunction with extensive CFD results.

As a consequence of mass continuity, jets occurring in C-V detrain air close to the outlet, a clear display of confinement effects, typically in the last third of its propagation path in the room (shown schematically in Figure 3, cases R and CR). Because there is mass rejection (or detrainment), the flow in this region cannot be classified as jet flow. The magnitude of the confinement effects in the flow can be scaled by comparing the characteristic jet diameter with the room dimensions. Typically, room surfaces are less than ten jet diameters away from the core of the jet at any point of its path in the room. As room dimensions tend toward two orders of magnitude bigger than the jet diameter, the jet tends toward free behavior (Hussein et al. 1994). In this case, the momentum flux in the recirculation flow becomes very small.

Figure 4 shows plots of mass and momentum flux variations in the room (both fluxes across the Y-Z plane) for the case plotted in Figure 2. As expected, from mass conservation principles, the mass flow rate in the return flow varies in proportion with the variations in the mass flow rate of the jet. The momentum fluxes show a similar behavior but, in this case, with more complex implications. The recirculation flux is a negative flux of negative momentum (negative X velocity). Therefore, both momentum fluxes are positive and increase simultaneously, resulting in a total momentum flux that has a maximum close to two-thirds of the way along the room. The pressure (not plotted) at the mid-plane level varies, as expected, in opposition to the momentum; a minimum occurs close to halfway along the room. When entering the room the jet is accelerated by a negative pressure gradient. Since the recirculation flow occurs in the opposite direction, this same pressure gradient also makes the recirculation flow stop. Air from the recirculation flow is entrained into the jet in a shear layer with a velocity scale U_{IN} (close to the inlet, the velocity of the recirculation flow is negligible). A positive pressure gradient occurs close to the outlet, an effect of the main jet flow reaching the outlet. This pressure gradient is associated with the deflection of part of the main jet, starting the recirculation flow.

This analysis of Figure 4 allows for a clearer picture of the flow behavior in the room. As the inlet jet propagates across the room, momentum is transferred to the room air, creating an entrainment-driven recirculation flow moving in the opposite direction, with a mass flow rate equal to the entrained flow in the main jet. The total momentum flux of the inflow jet is not constant: as the jet entrains, its momentum flux increases,

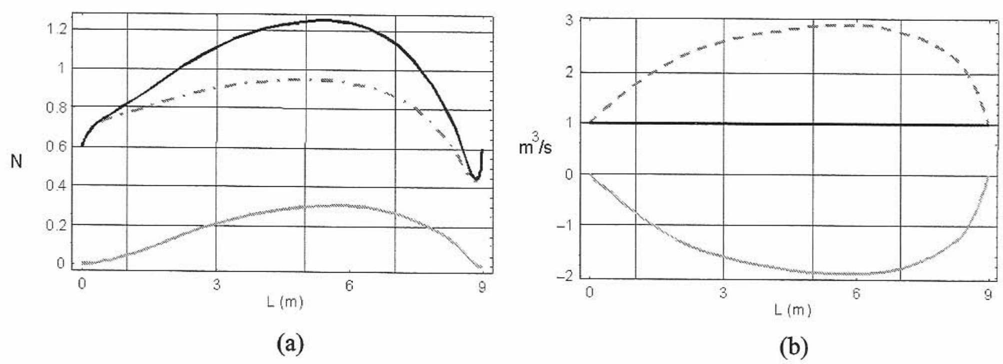

Figure 4 *Plots of momentum and mass flux variations for the case plotted in Figure 2. a) Momentum flux in the X direction across the cross section of the cross-ventilation flow (in Newtons). b) Mass flux of the flow—gray line: total flux in the recirculation region, black line: total in the flow.*

showing a similar trend to the momentum flux in the recirculation flow. Although the jet does not conserve its momentum (it is subjected to a significant pressure gradient), it seems that the recirculation inherits, in the mass rejection stage (close to the outlet), the momentum flux that occurs between the jet and the room air in the entrainment process.

We conclude that scaling wall currents in the recirculations with the inlet jet flow is the key to modeling recirculation flow. In particular, we identify the flux of momentum through the inlet aperture as the dominant flow feature and, the driving mechanism for the recirculation flow. This momentum flows into the room in the form of a jet whose characteristic dimension is typically not more than an order of magnitude smaller than the room length, resulting in a jet flow that is never fully developed and strongly confined.

SCALING LAWS FOR C-V AIRFLOW

If the correlation functions that will be developed are successful, it will be possible to obtain simple analytical expressions that characterize room airflow parameters (both in the main jet region and in the recirculation). In order to obtain the scaling relations, without solving the problem explicitly, the following approximations are used:

- Pressure variations inside the room are not considered. Although there is an assumption that pressure gradients scale with inlet momentum flux, the model will not explicitly include the pressure gradients in the correlation scaling.
- Variations in the momentum flux in the C-V direction will not be considered.
- Effects of drag on the indoor surfaces, and consequent energy dissipation, are not considered.
- It is considered that the jet never enters the transition stage before the mass rejection region close to the outlet; consequently, the jet can be modeled as a set of shear layers that develop in its perimeter and never intercept along the core of the jet.
- The analysis will only consider movements in the inflow direction. In some cases there are relevant movements in other directions particularly in rooms with offset apertures.
- The maximum room cross-sectional area occupied by the recirculation flow is considered to be a constant fraction of the total room cross-sectional area. The CFD simulation section shows that this fraction is close to one-half for a large array of common room geometries. In this way, the cross-sectional area of the recirculation flow is considered to scale with the room cross section.
- We will consider that all maximum values in the recirculation flow occur in the same location in the room, approximately two-thirds along the length, at the point where the main jet flow enters the detrainment stage. The maximum values that are relevant to the correlations are: the fractional area occupied by the flow, the average velocity, the momentum flux, and the mass flux.

Existing work on simple scaling of indoor airflows is well summarized in Etheridge and Sandberg (1996). No models exist for scaling recirculation flows. Jackman (1970) presented an experimentally validated scaling law, based on the existence of a direct scaling relation between inflow momentum flux and overall momentum flux in the room (without distinguishing regions in the flow). The scaling law predicts the average velocity inside rooms with small inlets and high ratio between momentum and mass fluxes (unlike the inlets considered in this study, windows and doors, that typically have small momentum to mass flux ratios). The inlet momentum flux scaling assumption proposed by Jackman (1970) forms the basis of one of the two scaling hypotheses that will be tested in this paper.

The inlet momentum flux is the source of the flow in the room, and the interface for inflow/room flow interaction is the shear that develops along the perimeter of the inflow jet. For this reason, inlet and shear layer momentum flux are candidate concepts to scale the momentum flux in the recirculation flow and will be tested using CFD simulations. After the momentum flux is scaled, all other relevant C-V scaling laws can be based on the momentum scaling principle used.

The inflow momentum flux-based scaling principle relies on the following sequence of assumptions: pressure variations in the room are proportional to the inlet momentum flux, and these pressure variations cause the changes in the return momentum flux of the room air in the recirculation regions. The result of this hypothesis is the following scaling relation between inlet and return momentum flux:

$$\Delta p \approx \rho A_R \cdot U_R^2 \Rightarrow A_R \cdot U_R^2 \approx A_{IN} \cdot U_{IN}^2 \Rightarrow U_R^2 = C_M A_{IN}/A_R \cdot U_{IN}^2 \tag{4}$$

The right side of Equation 4 is the product of a correlation constant, essential to make this simple analysis feasible, and a nondimensional function that depends on the system geometry parameters that are more influential in this balance of momentum fluxes (see function F in Equation 1; in this case, $F = A_{IN}/A_R$). The scaling function could have been obtained solely from dimensional analysis by composing a nondimensional multiplying factor using the three independent length scales in this problem:

1. The square root of the inlet area (see Equation 2).
2. The square root of the room cross section A_R.
3. The room length in the C-V direction, L.

A generic scaling function for this problem has the following form:

$$f = (\sqrt{A_{IN}})^m \cdot (\sqrt{A_R})^n \cdot L^p \tag{5}$$

When the correlation function f in Equation 4 is cast in this form, we obtain: $m = 2$, $n = -2$, and $p = 0$. There are infinite possible combinations of the variables in the exponent (m, n, and p) that ensure the necessary nondimensionality ($m + n + p = 0$). The shear layer based correlation hypothesis is obtained by using $m = 1$, $n = -2$, and $p = 1$, resulting in

$$U_R^2 = C_M \frac{\sqrt{A_{IN}^{1/2} \cdot L}}{A_R} \cdot U_{IN}^2 . \tag{6}$$

This scaling relation can also be obtained from simplified solution of the Navier Stokes equations by evaluating the momentum flux through the shear layer that develops in the perimeter of the inflow jet. The difference between Equations 6 and 5 is the replacement of the square root of A_{IN} by the room length L. According to the shear layer based correlation (Equation 6) longer rooms generate higher recirculation momentum fluxes (for similar A_{IN} and A_R).

By manipulating Equations 4 and 6 it is possible to obtain derived correlations for velocity and flow rate in the recirculation region. A correlation for evaluating occupant thermal comfort in this region can be obtained by defining an average velocity in the cross section of the room area that is occupied by recirculation flow (this area scales with A_R). Finally, multiplying the scaling relation for the average return velocity by the room cross-sectional area results in a correlation for the average flow rate. Starting from Equation 4 we obtain:

$$U_R = C_U \cdot \sqrt{\frac{A_{IN}}{A_R}} \cdot U_{IN} = C_U \cdot \frac{F_{IN}}{\sqrt{A_R \cdot A_{IN}}} \tag{7}$$

$$F_R \approx U_R A_R \Rightarrow C_F = C_F \sqrt{\frac{A_R}{A_{IN}}} \cdot F_{IN} \tag{8}$$

Similarly, for the correlation shown in Equation 6:

$$U_R = C_U \sqrt{\frac{A_{IN}^{1/2} L}{A_R}} U_{IN} = C_U \sqrt{\frac{L}{A_R \cdot A_{IN}^{3/2}}} F_{IN} \tag{9}$$

$$F_R \approx U_R A_R \Rightarrow F_R = C_F \sqrt{\frac{L A_R}{A_{IN}^{3/2}}} \cdot F_{IN} \tag{10}$$

In addition to these correlations, it is also useful to obtain a scaling relation for the average airflow velocity in the volume occupied by the main jet flow. For this correlation, inflow momentum scaling (Equation 4) will be used, an obvious choice given that this flow region is directly in front of the inlet:

$$A_R \cdot U_J^2 \approx A_{IN} \cdot U_{IN}^2 \Rightarrow U_J = C_{UJ} \cdot \frac{F_{IN}}{\sqrt{A_R \cdot A_{IN}}} \tag{11}$$

CFD SIMULATIONS

In order to test the correlations shown in Equations 4 and 6-10 and obtain the corresponding correlation constants that minimize the modeling error, a set of simulations of cross-ventilated rooms was performed. One of the main difficulties when using CFD is the choice and application of Reynolds averaged turbulence model (Wilcox 2000). Of the several models available, the k-ε model is a common choice because in most cases it can be sufficiently accurate and is relatively simple to use. Because the standard k-ε model is biased toward simplicity and computational efficiency, the region close to the solid boundaries is not solved numerically, as a way of avoiding the fine resolution needed to handle the high gradients that occur in these regions (in k, ε, and in the velocity parallel to the solid boundary (Wilcox 2000)).

In flows that are influenced by solid boundaries the use of wall functions can lead to significant errors. In order to avoid this error source, a low Reynolds number, near wall approach can be used, extending the numerical solution of the flow to the region close to the internal surfaces, by using a fine grid in the direction of the main flow gradients. The simulations presented here use the standard k-ε model in the core flow region (away from room surfaces) and the low Reynolds number model proposed by Lam and Bremhost (1981) close to the room surfaces. In a study by Henkes and Hoogendoorn (1989), this model was among the best low Reynolds number turbulence models (LRk-ε) for predicting velocity and temperature in a natural convection boundary layer.

The simulations were performed using a commercial CFD package. Simulations were considered converged when the normalized residuals were smaller than 10^{-3} and the solution field was stable (the values did not change by more than 10^{-7} (relative change) in each iteration and showed no visible fluctuation or changes after hundreds of iterations).

The results files of the simulations were post-processed in order to obtain the momentum flux in the recirculation flow and the other flow characteristics that will be correlated below. Results of simulations for different flow rates showed a linear variation of the velocities in the room with inlet velocity, as expected. As mentioned above, recirculation flow is characterized by negative X velocity. In order to define the jet region, a slightly different criteria was used to avoid the inclusion of the stagnation region that separates jet and recirculation. The fraction of the room volume occupied by the jet is calculated by adding all the room volumes where the X velocity at the cell center was bigger than one-tenth of the average inlet velocity, avoiding the inclusion of the stagnation regions.

Cases Simulated

Appropriate variations of the room geometry were used for all the parameters in the correlations. The values used must conform to the restrictions dictated by common applications in building ventilation as well as a set of restrictions imposed by the approximations in the model. The rules used were:

- The average inlet velocity should be lower than 2 m/s. This rule typically results in maximum velocities close to 1.5 m/s in the core of the room, a common upper limit imposed by comfort concerns in naturally ventilated spaces.
- The lower limit used for the average inlet velocity was 0.33 m/s. This limit results from two physical restrictions. First, for lower velocities, stagnation and other buoyancy-induced effects can have significant interference in the flow, changing the expected flow pattern that is the basis of the model. Second, turbulence-dominated conditions must be ensured in order for the correlations to apply. Natural ventilation flows usually meet or exceed this flow speed.
- Height: 2.25 m to 3.40 m; the lower limit is the common minimum height for a room. The upper limit corresponds to a tall room but does not reach the minimum height for a typical atrium. The model is not applicable to an atrium due to expected buoyancy effects that can change the flow pattern.
- Length: 2.25 m to 13.5 m; the lower limit is typical of small rooms. The upper limit ensures that simulated room jets will be in the developing region for most of the path in the room.
- Width: 2.25 m to 9 m; the lower limit ensures that the jet does not attach to the lateral surfaces and recirculation occur in the flow (one on each side of the main jet flow in the symmetric rooms). The upper limit ensures that the return flow has significant velocity.

Four types of inlets/outlets were used (see Table 1), two windows and two doors:

- A window, with dimensions 1 × 1 m, located at one-meter height (labeled: W).
- A wide window, with dimensions 2 × 1 m, located at one meter height (labeled: WW).
- A door, with dimensions 1 × 2 m (labeled: D).
- A wide door, with dimensions 2 × 2 m (labeled: WD).

Even when restricted to room geometries that conform to the limits described in this section, the variations in room dimensions, in conjunction with all possible inlet and outlet geometries, make testing the correlations a very extensive task. In order to make this task more manageable, the cases analyzed were restricted by choosing discrete values for each of the geometric parameters mentioned above. The different geometries and cases used in the simulations are presented in Tables 1 through 6.

TABLE 1
Dimensions of the Apertures Used to Develop and Test the Correlations

Aperture	Area (A_{IN}, m^2)	Perimeter (P, m)	Average Inlet Velocity (in m/s, for $F_{IN} = 1 m^3/s$)
Window (W)	1	4	1
Door (D)	2	5	0.5
Wide window (WW)	2	6	0.5
Wide door (WD)	4	6	0.25

TABLE 2
Dimensions of the Rooms Used to Develop and Test the Correlations

Case	21	122	123	221	222	223	141	142	143	144	146	241	242	243	244	246
H (m)	2.25	2.25	2.25	3.5	3.5	3.5	2.25	2.25	2.25	2.25	2.25	3.5	3.5	3.5	3.5	3.5
W (m)	4.5	4.5	4.5	4.5	4.5	4.5	9	9	9	9	9	9	9	9	9	9
L (m)	2.25	4.5	6.75	2.25	4.5	6.75	2.25	4.5	6.75	9	13.5	2.25	4.5	6.75	9	13.5
Vol. (m^3)	23	46	68	35	71	106	46	91	137	182	273	71	142	213	284	425
A_R (m^2)	10	10	10	16	16	16	20	20	20	20	20	32	32	32	32	32

TABLE 3
Subset of Cases Used to Develop the Main Correlations ($1<C_L<4$). A_F is the Minimum Room Cross-Sectional Fraction Occupied by the Recirculation Flow

Case	D122	D123	D142	D143	D144	D146	D222	D223	D242	D243
C_L	2.6	3.9	1.1	1.7	2.3	3.4	2.6	3.9	1.1	1.7
A_F	0.57	0.55	0.54	0.55	0.54	0.53	0.64	0.71	0.53	0.53
Case	**D244**	**D246**	**W121**	**W122**	**W123**	**W142**	**W143**	**W144**	**W146**	**W221**
C_L	2.3	3.4	1.3	2.6	3.9	1.1	1.7	2.3	3.4	1.3
A_F	0.52	0.53	0.52	0.53	0.56	0.52	0.52	0.52	0.51	0.50
Case	**W222**	**W223**	**W242**	**W243**	**W246**	**WD122**	**WD142**	**WD143**	**WD144**	**WD146**
C_L	2.6	3.9	1.1	1.7	3.4	3.6	1.3	1.9	2.6	3.9
A_F	0.49	0.50	0.49	0.50	0.49	0.62	0.57	0.55	0.55	0.55
Case	**WD246**	**WW122**	**WW142**	**WW143**	**WW144**	**WW146**	**WW242**	**WW243**	**WW244**	**WW246**
C_L	3.9	3.6	1.3	1.9	2.6	3.9	1.3	1.9	2.6	3.9
A_F	0.51	0.69	0.55	0.54	0.54	0.53	0.54	0.53	0.52	0.51
Case	**W124**	**W126**	**W224**	**W226**	**WW123**	**WW124**	**WW126**	**WW224**	**WW226**	**D124**
C_L	5.1	7.7	5.1	7.7	5.4	7.2	10.8	7.2	10.8	5.1
A_F	0.47	0.47	0.48	0.49	0.64	0.62	0.63	0.58	0.57	0.52
Case	**D126**	**D224**	**D226**	**WD123**	**WD124**	**WD126**				
C_L	7.7	5.1	7.7	5.4	7.2	10.8				
A_F	0.53	0.68	0.63	0.60	0.60	0.60				

TABLE 4
Subset of Cases Used to Develop the Correlations for Long Rooms ($C_L>4$)

Case	W124	W126	W224	W226	WW123	WW124	WW126	WW224
C_L	5.1	7.7	5.1	7.7	5.4	7.2	10.8	7.2
A_F	0.47	0.47	0.48	0.49	0.64	0.62	0.63	0.58
Case	**WW226**	**D124**	**D126**	**D224**	**D226**	**WD123**	**WD124**	**WD126**
C_L	10.8	5.1	7.7	5.1	7.7	5.4	7.2	10.8
A_F	0.57	0.52	0.53	0.68	0.63	0.60	0.60	0.60

The model presented in this paper only applies when the flow pattern is dominated by forced convection. For typical rooms, this will occur whenever the room height is ≤3.5 m and the temperature variations between inlet and outlet are smaller than ≈2°C. When strong buoyancy effects are present in the flow, the horizontal recirculations can become undefined and have different characteristics. This case is not treated in this paper.

All the room geometries used to develop the correlation have one inlet and one outlet, with the same dimensions, placed in the center of the inlet and outlet surfaces (the door is placed in the center on the horizontal and adjacent to the floor on the vertical). The horizontal symmetry of all the cases allowed for the simulation of only one-half of the flow domain, simplifying the simulations (see Figure 2).

The model may still be applicable to rooms outside these limits as long as all of the following conditions are verified:

- Most of the jet path in the room is in the shear layer region (the jet does not enter the transition region before two-thirds of the room length).
- Buoyancy sources, such as vertical heated or cooled room surfaces, do not dominate the flow.
- The flow is turbulent in the jet region and in the boundary layers close to the room surfaces in the recirculation regions.

The cases simulated were labeled using one letter for the aperture type (W, WW, D, and WD), and three numbers for the height, width, and length. The numbers used for the room dimensions are scaled with room height. The number two is

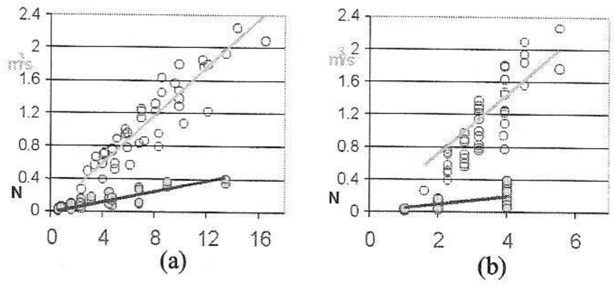

Figure 5 *a) Correlation lines for shear layer based circulation momentum flux (black line) and mass flow rate (gray line), b) correlation lines for inlet momentum flux based circulation momentum flux (black line) and mass flow rate (gray line). In both cases the CFD post-processed results for the cases shown in Table 3 (gray dots for the momentum flux and circles for mass flow rate).*

used to label the height in the cases with 3.40 m height for simplicity. All cases where simulated using a one cubic meter per second volumetric flow rate. For all the inlets a turbulence-dominated airflow pattern can be obtained for flow rates of 0.5 m^3/s and even lower in the case of the standard window and door (see Table 1). It is important to use similar flow rates for all rooms and aperture types in order to allow for straightforward comparisons between the recirculation flows that result from different geometries.

RESULTS AND ANALYSIS

The correlation constants (C_F, C_M, C_U, and C_{UJ}) on the right hand side of Equations 4 and 6-11 were determined using linear regression. The obtained linear regression lines (that always pass through the origin) are plotted against the post-processed CFD results for the correlated quantities in Figures 5a and 5b, showing the maximum of the momentum and mass fluxes in the recirculation regions as a function of the right-hand side of Equations 4 and 8 (Figure 5a) and 6 and 10 (Figure 5b).

The momentum flux in the recirculation occurs through a fraction of the cross-sectional area, with the reminder occupied by the jet flow. Table 3 shows the designations of the 46 cases used to develop the main correlations. In this table, the line labeled A_F shows the fraction of the room cross-sectional area occupied by the jet in the point of maximum mass flow rate. Although there is noticeable variation in the values of minimum 0.47, maximum 0.71, most values are close to 0.5. We conclude that, within the first order precision goal, the area occupied by the recirculation flow can be scaled using A_R (any constant multiplying value, such as one-half, is unimportant and will be included in the correlation constants). The adequacy of this and all other approximations is tested in the correlations presented.

Qualitative analysis of Figure 5 shows that the shear layer based correlation is more adequate; in addition, the correlation constant R^2 for the shear layer case is significantly higher than the inlet momentum flux ($R^2=0.75$ versus $R^2=0.44$, see Table 6). Clearly, for the set of cases used in this study, shear layer principles are more effective than inlet momentum flux scale, the momentum flux of the recirculation flow. The gray lines in Figure 5 represent the recirculation mass flow rate correlations (labeled $C_F(10)$ and $C_F(8)$ in Table 6); again, analysis of this figure confirms the better results from the shear layer based correlations (from Equations 6 and 10).

TABLE 5
Subset of cases with 1/3< C_L < 1

Case	D141	W141	WD141	W241
C_L	0.6	0.6	0.6	0.6
A_F	0.54	0.53	0.55	0.47

Tables 4 and 5 show a set of 20 additional cases where the flow has a different balance, although still characterized by two distinct regions. The common characteristic of the 16 cases, shown in Table 4, is a large length to width ratio. In these cases, the flow eventually attaches to the lateral surfaces in the region close to the outlet in the last third of the room length. The flow starts with recirculations but toward the outlet becomes similar to case C, where the momentum flux in the room scales with inlet momentum flux. Further, the maxima of the recirculation flow parameters (momentum, mass, and velocity) occur in the first half of the room (as opposed to two-thirds or further along the room). Due to their combined nature, partially type R, partially type C, these cases have different slopes in the momentum flux correlations (see correlations labeled (*) in Table 6). Further, due to the transition between recirculation and attached flow that occurs in these cases, the flow pattern is expected to be particularly sensitive to furniture and buoyancy effects that are always present in real rooms. Table 5 shows four cases where the flow balance is also different from the main set of cases shown in Table 3. In these cases the width to length ratio is large, making the recirculation behave differently, with a small momentum flux (due to the small room length) occurring in a relatively large cross-sectional area.

Clearly, it is essential to develop a simple criterion to distinguish standard C-V recirculation cases from these transitional cases. The criteria that most successfully achieves this distinction is

$$C_L = \frac{2L}{W - W_{IN}}, \qquad 1 \le C_L \le 4 . \qquad (12)$$

The values of C_L are shown in Tables 3 to 5 for each case (lines labeled C_L). Note that C_L is 4, the transition value, corresponding to rooms with a length to width ratio of less than 2 (depending on the width of the inlet). The ratio on the right-hand side of Equation 12 scales the growth of the shear layer that develops at the limit of the main jet flow (proportional to L) with the available room width for shear layer expansion (on the denominator). The use of the width as the length scale for available space for shear layer expansion reflects the low

TABLE 6
Results of the Correlations

Correlation	$C_M(6)$	$C_M(4)$	$C_U(9)$	$C_U(7)$	$C_U(9)$*	$C_U(7)$*	$C_F(10)$	$C_F(8)$	$C_F(10)$*	$C_F(8)$*	$C_{UJ}(11)$
Best Fit Slope	0.032	0.209	0.298	0.680	0.162	0.487	0.147	0.360	0.077	0.231	1.558
Linear Regression R^2	0.75	0.44	0.67	0.42	0.28	0.55	0.88	0.71	0.89	0.83	0.96
Max/Min	27.5	27.5	4	4	3.7	3.7	10.6	10.6	4.6	4.6	3.6
Average Error (%)	30	60	16	19	19	60	17	28	17	92	5
Maximum Error (%)	111	267	38	72	64	149	55	110	51	163	13

The corresponding equation number is shown in parenthesis. The columns signaled with (*) are for C_L>4. All lines pass by the axis origin. The line labeled max/min shows the ratio between minimum and maximum values obtained from the library of CFD cases used to develop the correlation.

height to width ratio of the rooms used in the CFD simulations, which leads to jet attachment to part of the floor and ceiling surfaces that are directly in front of the aperture, limiting its vertical expansion. In the case of a room with height comparable to the width, it is more appropriate to use a scaling principle based on characteristic diameters of the room cross-section and inlet aperture areas.

One important fact displayed by Equation 12 is that rooms where the inlet is placed close to one of the lateral surfaces tend to have more space for shear layer growth. This leads to higher recirculation mass flow rates and velocities. When evaluating these rooms using criteria 12, the factor of two in the denominator must be dropped.

It will be shown below that the flow pattern for cases with C_L bigger than 4 can also be correlated with similar principles, although requiring different correlation constants. The cases in Table 5 (C_L<1) were not used to develop the main correlations but are reasonably modeled by these correlations. The correlations are expected to be very imprecise for cases with C_L <1/3 and C_L >11.

The lower limit imposed on C_L already indicates that the model should not be applied when the aperture size is much smaller than the room characteristic length, meaning the model should only be used when

$$\sqrt{A_{IN}} > \frac{\sqrt[3]{L \cdot W \cdot H}}{10}. \qquad (13)$$

When the system geometry does not conform to this last criteria, the jet can enter the transition stage while inside the room and many of the approximations explained above are not applicable.

Table 6 shows the slopes of the lines that minimize the error for the correlations described above (these slopes are the correlation constants). From the results shown in this table it is possible to conclude that the correlations proposed achieve first order accuracy. Note that only five of the eleven correlations shown in the Table 6 are adopted in the model, they are:

1. Average recirculating flow velocity in the room cross section with maximum flow rate (1/3 < C_L < 11):

$$U_R = C_U\sqrt{\frac{L}{A_R \cdot A_{IN}^{3/2}}}F_{IN}, \qquad C_U = \begin{cases} 0.298, & 1/3 \le C_L \le 4 \\ 0.162, & 4 < C_L \le 11 \end{cases} \qquad (14)$$

2. Average volumetric velocity in the main jet region (1/3 < C_L < 11):

$$U_J = 1.56\frac{F_{IN}}{\sqrt{A_R \cdot A_{IN}}}, \qquad 1/3 \le C_L \le 11 \qquad (15)$$

3. Volumetric flow rate of the return flow (1/3 < C_L < 11):

$$F_R = C_F\sqrt{\frac{LA_R}{A_{IN}^{3/2}}} \cdot F_{IN}, \qquad C_F = \begin{cases} 0.147, & 1/3 \le C_L \le 4 \\ 0.077, & 4 < C_L \le 11 \end{cases} \qquad (16)$$

Not surprisingly, the best correlation is for the average velocity in the jet region, successfully predicting a set of cases that has a relative variation of 3.6 (Max/Min line in Table 6), with negligible error. It is interesting to see how accurate the simple shear layer based correlation (Equation 6) is when estimating momentum flux in the cases shown in Table 3. This correlation, obtained from Equation 6 (labeled $C_M(6)$ in Table 6), can predict the momentum flux with an average error of 30% for a set of CFD post-processed values with a maximum variation of 27.5 in magnitude. It is relevant to note that the relative errors do not depend on the flow rate. Any interval of flow rate values linearly increases the prediction intervals shown in the fourth line of Table 6, making the final results of the model more impressive.

The correlations labeled with a (*) in this table refer to the cases with $C_L > 4$ (long rooms, shown in Table 4). As expected, the slopes in these correlations are always smaller than for the standard correlations (cases in Table 3), as a consequence of the higher dissipation that occurs in long rooms.

Applications to C-V Design

In addition to the correlation expressions presented above, when designing cross-ventilated rooms two additional ratios can be useful: the ratio between maximum velocity in the room and velocity in the main jet region and the ratio between velocity in this region and velocity in the recirculation.

The first ratio is important whenever a designer must limit the maximum air velocity at any point in the room. The maximum velocity always occurs directly in front and close to the inlet, in the vena contrata region. The fractional contraction of the jet (coefficient C_D) is due to the flow through the inlet and can be obtained analytically for a two-dimensional flow, with measurements in three-dimensional flows resulting in similar values (Ohba et al. 2001). The maximum velocity and the desired ratio are given by:

$$U_M = \frac{F_{IN}}{A_{IN}C_D}, \qquad C_D = 0.611$$
$$\frac{U_J}{U_M} = 1.56 C_D \sqrt{\frac{A_{IN}}{A_R}}, \qquad 1/3 \le C_L \le 11 \tag{17}$$

In some situations the maximum room airflow velocity is a limitation on the design and maximizing the second relation in Equation 17 results in a ventilation system with higher velocities in the jet region of the room while remaining below the maximum allowed velocity ($U_J/U_M<1$, as can be seen in Figure 6a).

The second relevant ratio is between velocities in the jet region and in the recirculation region, given by:

$$\frac{U_R}{U_J} = C_R \sqrt{\frac{L}{A_{IN}^{0.5}}} \qquad C_R = \begin{cases} 0.191, & 1/3 \le C_L \le 4 \\ 0.104, & 4 \le C_L < 11 \end{cases} \tag{18}$$

This ratio is always smaller than one and independent of the room cross-sectional area. Figure 6b shows plots of Equation 18 for variable inlet areas and room lengths. Longer rooms maximize this ratio up to a limiting length since the flow pattern limitations translated in the criteria shown in Equations 12 and 13 must be respected.

Figure 7a shows the ratio between inlet flow rate and the recirculation flow rate predicted using Equation 16 for cases with $C_L<4$. It is interesting to note that for rooms with moderate to large volumes and inlets with areas below 2 m^2 this ratio is bigger than one and can even reach three. These high recirculation flow rates are achieved with the above mentioned small momentum fluxes, when compared with the inlet flow, because the flow occurs in a large area, approximately one-half of the room cross section (see Table 3, line: A_F).

Figure 7b illustrates possible advantages of using the model in conjunction with other models, in this case the Fanger thermal comfort model (ISO 1993). The impacts of room geometry and flow rate variations on summer cooling, due to increased air movement, are easily quantified. As expected, higher flow rates and smaller inlet areas result in higher velocities and increased thermal comfort.

So far this paper has discussed symmetric rooms or rooms with part of the inlet and outlet perimeters adjacent to the same lateral surface. Asymmetric rooms are very common. Limited, exploratory simulations for a few of the cases shown in Table 3, using asymmetric inlet/outlet configurations, indicate that the model and the correlations presented above are directly applicable to asymmetric rooms (where the inlet does not face the outlet). It should be noted that in these rooms the smaller of the two recirculation regions tends to have a higher velocity and also reach values of C_L>4 for smaller length to width

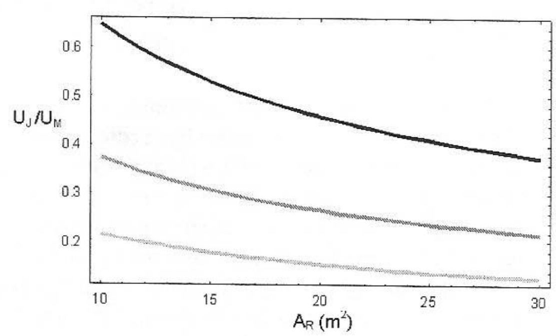

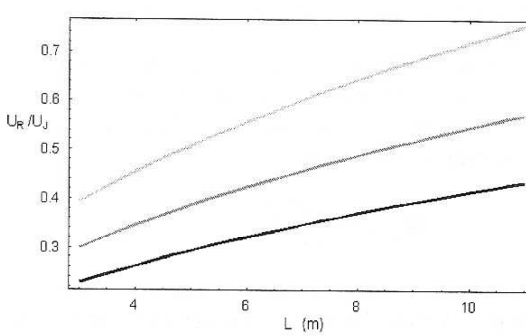

Figure 6 *a) Variation with room cross-sectional area (A_R) of the raio between the average velocity in the jet region and the maximum velocity in front of the inlet (expression 25). b) Variation with room length (L) of the ratio between the average velocity in the recirculation and in the jet region (expression 26). In both plots, three inlet sizes are used: 0.5 m^2 (light gray), 1.5 m^2 (medium gray), and 4 m^2 (black).*

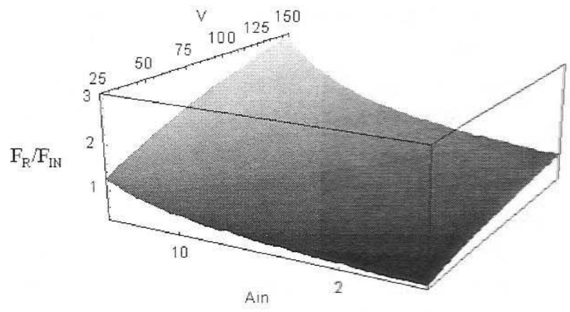

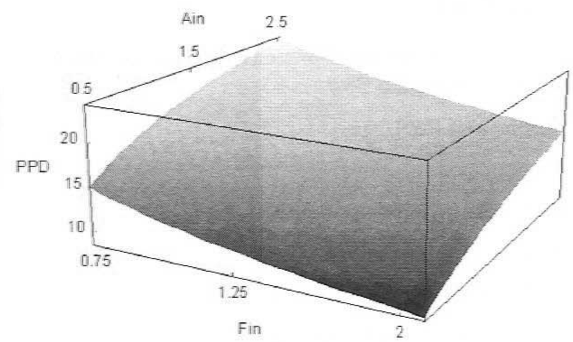

Figure 7 *a) Ratio between the recirculation mass flow rate* F_{RS} *(expression 24) and the inlet volumetric flow rate* (F_{IN}) *for variable room volume (V in* m^3*) and inlet aperture area* (A_{IN} *in* m^2*). b) Percentage of people dissatisfied in the recirculation region of a cross-ventilated room for variable volumetric flow rate* (F_{IN} (m^3/s)) *and inlet aperture area* (A_{IN} (m^2)), *calculated using Fanger's comfort model (ISO 1993). Calculation performed using* $L = 8$ *m,* $T = 27.5°C$, *and* $A_R = 15$ m^2, *with a metabolic rate of 1.5 met and standard summer clothing (ASHRAE 2001).*

ratios. In order to correctly apply the correlation principles to these rooms, each recirculation zone should be analyzed independently, applying the correlation formulas twice and using different areas and room widths on each side, a more cumbersome procedure. In this context, for design estimation purposes, the authors recommend the use of the standard correlations, keeping in mind that the results will be less precise.

One last geometric element that is present in most rooms is furniture. Large furniture can change the flow pattern and the recirculation flow characteristics. One straightforward approach to including furniture effects is to define an equivalent room cross-sectional area, obtained by subtracting the characteristic furniture obstruction area from A_R. Still, it is only a first order estimation of the effects that may, or may not, be applicable depending on the room. The authors will attempt to include general effects of furniture in future developments of the model. The present model should not be used for estimating flow characteristics in rooms where multiple large size floor standing furniture elements occupy more than a third of the room volume or when the inflow jet path is obstructed by furniture.

Using this model in a generic ventilation flow requires several steps:

- First, the user must make sure that the room has an inlet facing the outlet, a geometry that leads to C-V.
- Second, the criteria shown in Equation 13 must be satisfied, ensuring significant momentum conservation.
- Third, the flow must be dominated by forced convection; for typical rooms, this will occur whenever the room height is ≤3.5 m and the temperature variation between inlet and outlet is smaller than ≈2°C.
- Fourth, A^* must be calculated; whenever $A^* \leq 2$ recirculations occur, and if $1/3 \leq C_L \leq 11$, then Equations 14-18 can be used to obtain the magnitude of the velocities and flow rates in the two main flow regions. Whenever $A^* \cong 1$ the flow resembles flow in a pipe with a single region (main jet) and modeling is straightforward and does not require correlations.

CONCLUSIONS

The C-V model developed in this paper meets the proposed first order precision goal while retaining simplicity in its form and application. A simple criterion is introduced, Equation 13, that assesses the existence of significant momentum conservation and, therefore, C-V, in isothermal flows. Two further criteria are introduced, Equations 3 and 12, allowing for straightforward distinction between different types of C-V flows. The correlations shown in Equations 14-18 model several useful flow parameters in a simple way, making design and control of C-V systems a simpler task.

The obtained equations and criteria clearly display the effects of the most relevant system geometric parameters and provide simple insight into the mechanisms that control the complex C-V airflow. The functional dependences of the flow characteristics on the different room geometry parameters where clearly identified.

Future developments of the model are: simplified modeling of asymmetric rooms and furniture effects as well as extension of the present method to analyze heat and pollutant transfer in cross-ventilation airflows.

The present study should allow for improved understanding of C-V flows and contribute to their increased use, which should lead to reductions in building energy consumption and improved control and confidence in the performance of C-V systems.

NOMENCLATURE

A_F = minimum room cross-sectional fraction occupied by the recirculation flow

A_{IN} = inlet area (m^2)

A_R = room cross-sectional area (m^2).

A^* = nondimensional room area ratio

C_F = flow rate correlation constant.

C_L = flow scaling nondimensional criterion

C_M = momentum correlation constant

C_n = dimensionless correlation constant (the index n distinguishes different correlated variables)

C_R = correlation constant for the ratio between jet and recirculation velocity

C_U = velocity correlation constant

C_{UJ} = correlation constant for the average velocity in the room volume occupied by inlet jet flow

F = scaling law function

f = inlet flow profile function

F_{IN} = inlet flow rate (in m^3/s, given by $U_{IN} \cdot A_{IN}$)

F_R = flow rate in the recirculation region (m^3/s)

M = momentum flux of the jet (in N or J/m)

P = perimeter of the inlet aperture (m)

U_J = average velocity in fraction of the room volume occupied by inlet jet flow (m/s)

U_M = maximum velocity in the room (m/s)

U_R = averaged velocity in a given region of the room that is being modeled (m/s)

W_{IN} = width of the inlet aperture (m)

ACKNOWLEDGEMENTS

The authors would like to acknowledge the financial support of the Fundação para a Ciência e Tecnologia (Lisbon, Portugal) and the California Energy Commission's Public Interest Energy Research (PIER) Buildings Program. The authors would also like to thank Professors Colm Caulfield, Edward Arens, and Doctor Philip Haves for providing valuable input to the work presented in this paper.

REFERENCES

Allard, F., and C. Inard. 1992. Natural and mixed convection in rooms, Prediction of thermal stratification and heat transfer by zonal models. Proceedings of ISRACVE, pp. 335-342, Tokyo, 1992.

ASHRAE. 2001. *2001 ASHRAE Handbook—Fundamentals*, Chapter 25. Atlanta: American Society of Heating, Refrigerating and Air-Conditioning Engineers, Inc.

Aynsley, R.M., W. Melbourne, and B. Vickery. 1977. *Architectural Aerodynamics*. London: Applied Science Publisher.

Baturin, V.V., and N.S. Billington. 1972. *Fundamentals of Industrial Ventilation*. Franklin Book Company, pp. 174-179.

Bejan, A. 1994. *Convection Heat Transfer,* 2d ed. Wiley.

Ernest, D.R., F.S. Bauman, and E.A. Arens. 1991. The prediction of indoor air motion for occupant cooling in naturally ventilated buildings. *ASHRAE Transactions* 97(1): 539-552.

Etheridge, D., and M. Sandberg. 1996. *Building Ventilation: Theory and Measurement*. England: John Wiley & Sons.

Givoni, B. 1976. *Man, Climate and Architecture*, 2d ed. New York: Van Nostrand Reinhold.

Henks R.A.W.M., and C.J. Hoogendoorn. 1989. Comparison of turbulence models for the natural convection boundary layer along a heated vertical plate. *International Journal of Heat and Mass Transfer* 32: 157-169.

Hussein, H.J., S.P. Capp, and W.K. George. 1994. Velocity measurements in a high-Reynolds-number, momentum-conserving, axisymmetric, turbulent jet. *Journal of Fluid Mechanics* 258:31.

ISO. 1993. Moderate Thermal environments—Determination of the PMV and PPD indices and specifications for thermal comfort. *International Standard 7730.*

Jackman, P. 1970. Air movement in rooms with sill mounted griles—a design procedure. Laboratory report no. 65, Bracknell, U.K.

Lam C.K.G., and K. Bremhost. 1981. A modified form of the K-ε model for predicting wall turbulence. Transactions of ASME, *J. Fluids Eng.* 103: 456-460.

Malmstrom, T.G., A.T. Kirkpatrick, B. Christensen, K. Knappmiller. 1997. Centerline velocity decay measurements in low-velocity axisymmetric jets. *J. Fluid Mech.* pp. 346, 363.

Neiswanger, L., G.A. Johnson, and V.P. Carey. 1987. An experimental study of high Raleigh number mixed convection in a rectangular enclosure with restricted inlet and outlet openings. *Transactions of ASME*, 109: 446-453.

Ohba, M., K. Irie, and T. Kurabuchi. 2001. Study on airflow characteristics inside and outside a cross-ventilation model, and ventilation flow rate using wind tunnel experiments. *Journal of Wind Engineering and Industrial Aerodynamics*, in press.

PHOENICS Version 3.3. 2000. London: CHAM Ltd.

Tennekes, H., and J.L. Lumley. 1994. *A First Course in Turbulence*. Cambridge, Mass.: The MIT Press.

Wilcox, DC. 2000. Turbulence modeling for CFD. DCW Industries, La Canada.